Efficient Compressive Sensing of ECG Segments Based on Machine Learning for QRS-Based Arrhythmia Detection

Jeevan K. Pant and Sridhar Krishnan
Department of Electrical and Computer Engineering, Ryerson University
Toronto, ON, M5B 2K3, Canada
Email: {jeevan1.pant,krishnan}@ryerson.ca

***Abstract*— A novel method for efficient telemonitoring of arrhythmia based on using QRS complexes is proposed. Two features, namely, sum of absolute differences (SAD) and maximum of absolute differences (MAD) are efficiently computed for each ECG segment in the bio-sensor. The computed features can be transmitted from the bio-sensor using wireless channel, and they can be used in the receiver for determining the absence of QRS complex in the segment. By avoiding computationally expensive signal reconstruction for the ECG segments without QRS complex, it is shown, using simulation results, that computation time can be reduced by approximately 7.4% for long-term telemonitoring of QRS-based arrhythmia. Detection of the absence of QRS complex can be carried out in around 7 milliseconds in a standard laptop computer with 2.2GHz processor and 8GB RAM.**

I. INTRODUCTION

Arrhythmia detection based on the locations of QRS complexes is an important process in ECG signal processing, where portable wireless bio-sensors offer convenient ways for measuring ECG signals from a subject when he/she is performing various types of activities [1]–[4]. Such bio-sensors are usually battery operated, where low power-consumption is highly desired. Compressive sensing (CS) is a technique for the acquisition of sparse signals [5], and signal reconstruction in CS can be carried out by using the algorithms [6], [7], whose expensive computational complexity has been well recognized. Recently, the algorithms tailored for the reconstruction of biomedical signals are found to offer effective CS in biomedical engineering applications [8]–[12]. Yet, further reduction in the computational effort required for signal reconstruction is highly desired.

In this paper, we propose a method for reducing computational effort for compressive sensing of ECG signals for the telemonitoring of QRS complexes. For an ECG segment, two features, namely, the sum of absolute differences (SAD) and maximum absolute difference (MAD), are efficiently computed at the sensor unit and transmitted as two additional components of the measurements of the ECG segment. In the receiver, the features are used to detect the ECG segments without QRS complex, called as the non-QRS ECG segment, which may contain a P wave, a T wave, isoelectric line, low-amplitude head of Q wave, and/or low-amplitude tail of S wave. For a non-QRS ECG segment, computationally expensive signal reconstruction algorithm is not applied, and the zero-vector is used as the reconstructed segment. Thus, computational effort required for monitoring QRS complexes over a long period of time can be reduced. A machine learning based algorithm, such as support vector machine (SVM) algorithm, can be used for the detection of the non-QRS ECG segments. Simulation results indicate that machine learning can be carried out very efficiently; classification can be carried out even more efficiently.

II. BACKGROUND

In compressive sensing (CS), a total of M measurements $\boldsymbol{y}$ and signal vector $\boldsymbol{x}$ of length N are interrelated as

$$\boldsymbol{y} = \boldsymbol{\Phi x} \tag{1}$$

where $\boldsymbol{\Phi}$ is a measurement matrix of size $M \times N$.

The ℓ_p^d-regularized least-squares (ℓ_p^d-RLS) [13], ℓ_p^{2d}-regularized least-squares (ℓ_p^d-RLS) [11], and $\ell_{2/p}^d$-regularized least-squares ($\ell_{2/p}^d$-RLS) [9] algorithms for the reconstruction of $\boldsymbol{x}$ from $\boldsymbol{y}$ are based on solving the problem

$$\underset{\boldsymbol{x}}{\text{minimize}} \quad \tfrac{1}{2}\,||\boldsymbol{\Phi x} - \boldsymbol{y}||_2^2 + \lambda f(\boldsymbol{x}) \tag{2a}$$

with

$$f(\boldsymbol{x}) = \sum_{i=1}^{N-1} \left[\left(x_i^d\right)^2 + \epsilon^2 \right]^{p/2}, \tag{2b}$$

$$f(\boldsymbol{x}) = \sum_{i=1}^{N-2} \left[\left(x_i^d - x_{i-1}^d\right)^2 + \epsilon^2 \right]^{p/2}, \tag{2c}$$

and

$$f(\boldsymbol{x}) = \sum_{i=1}^{S} \left(\left|\tilde{x}_i^d\right|^2 + \epsilon^2 \right)^{p/2}, \tag{2d}$$

respectively. They are found to be effective for the reconstruction of physiological signals, including ECG signals and foot-gait signals. In (2), x_i^d is the ith component of the first-order difference vector $\boldsymbol{x}^d$ constructed as

$$\boldsymbol{x}^d = \begin{bmatrix} x_1^d & x_2^d & \cdots & x_{N-1}^d \end{bmatrix}^T$$

where $x_i^d = x_i - x_{i+1}$, for $i = 1, 2, \ldots, N-1$. In (2d), $\tilde{x}_1^d$, $\tilde{x}_2^d$, …, $\tilde{x}_S^d$ are the blocks of the vector $\boldsymbol{x}^d$, where each block is of length b so that $N = Sb + 1$, see [9] for more discussion.

978-1-4577-0220-4/16/$31.00 ©2016 IEEE

III. DETECTION OF NON-QRS ECG SEGMENTS

SAD and MAD features for an ECG segment $\boldsymbol{x}$ of length N, denoted as f_1 and f_2, can be evaluated using

$$f_1(\boldsymbol{x}) = \sum_{n=1}^{N-1} |x_n - x_{n+1}|, \tag{3}$$

and

$$f_2(\boldsymbol{x}) = \underset{1 \le n \le N-1}{\text{maximum}} |x_n - x_{n+1}|, \tag{4}$$

respectively. Block-diagram of the proposed circuit for the computation of f_1, f_2 is shown in Fig. 1. Samples x_1, ..., x_N can be sequentially supplied to the circuit as they become available. The circuit stores the ith sample in a temporary memory for the sampling interval and subtracts it from the $(i+1)$th sample. The `ABS()` block computes $|x_i - x_{i+1}|$. The `Accumulator` block accumulates the sequence of values coming from the `ABS()` block. The `Max. Selector` block determines the maximum value in the sequence. Outputs of the `Accumulator` and `Max. Selector` blocks are read as the features f_1 and f_2 after the last sample x_N is used for the computation.

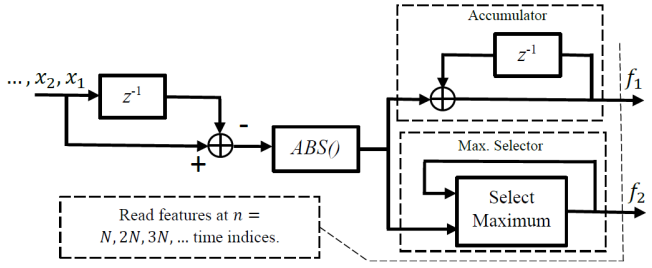

Fig. 1. Block diagram of the proposed circuit for computing the features f_1, f_2.

While computing f_1, f_2, M measurements $\boldsymbol{y}$ are also obtained by using a different circuit implemented for performing the CS operation (1). Features f_1 and f_2 can be included in the vector $\boldsymbol{y}$ as additional components to construct a data frame. Components of the data frame can be sequentially transmitted from the bio-sensor through a wireless channel. A receiver would read the frame and forward it to the signal reconstruction process, whose block diagram is shown in Fig. 2. Features f_1, f_2 are extracted from the frame, and classification operation `CLASS` is applied on it to determine whether $\boldsymbol{x}$ is a non-QRS ECG segment or not. If $\boldsymbol{x}$ is a non-QRS ECG segment, signal reconstructed algorithm is not applied and the zero-vector is used as the reconstructed signal $\hat{\boldsymbol{x}}$.

The `CLASS` operation in Fig. 2 can be implemented by using a machine-learning-based feature classification technique. By using the `CLASS` operation and bypassing the signal reconstruction step for non-QRS ECG segments, computational effort required for the long-term detection of the QRS complexes can be reduced.

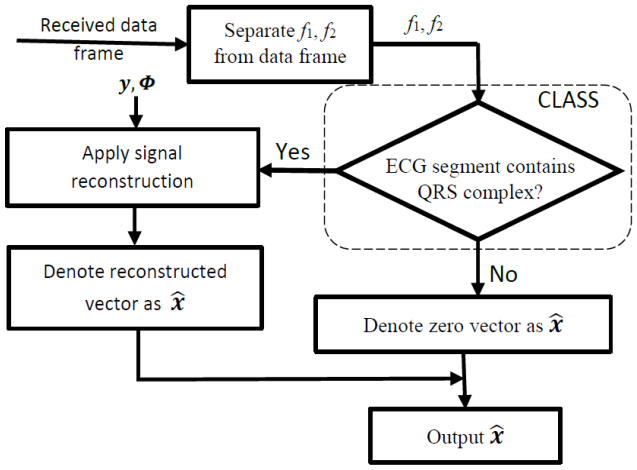

Fig. 2. Block diagram of the proposed signal reconstruction process.

A. Complexity Analysis for Feature Computation

Let $\boldsymbol{\Phi}$ be a random sparse matrix of size $M \times N$, each column of $\boldsymbol{\Phi}$ has five unity-valued components, and the rest of the components in the columns of $\boldsymbol{\Phi}$ are zero-valued. The five unity valued components in a column of $\boldsymbol{\Phi}$ are randomly located. Suppose A_1, A_2, ..., A_M be the memory addresses used to store the components of $\boldsymbol{y}$ in a bio-sensor and $a_{1,i}$, $a_{2,i}$, $a_{3,i}$, $a_{4,i}$, $a_{5,i}$ for $i = 1, 2, \ldots, N$ be the memory addresses where the indices of the unity-valued components of the ith column of $\boldsymbol{\Phi}$, for $i = 1, 2, \ldots, N$, are stored. If components x_1, x_2, ..., x_N of $\boldsymbol{x}$ become available in sequence, the CS operation (1) can be implemented in the bio-sensor by using the following procedure.

1. Reset memory locations A_1, A_2, ..., A_M to zero values.
2. For $i = 1, 2, \ldots, N$:
   - 2.a Read incoming sample x_i.
   - 2.b Read indices i_1, i_2, i_3, i_4, i_5 from the addresses $a_{1,i}$, $a_{2,i}$, $a_{3,i}$, $a_{4,i}$, $a_{5,i}$, respectively.
   - 2.c Read i_1th, i_2th, i_3th, i_4th, i_5th components of $\boldsymbol{y}$ from memory locations A_{i_1}, A_{i_2}, A_{i_3}, A_{i_4}, A_{i_5}.
   - 2.d Add x_i to each of the five components of $\boldsymbol{y}$, read in the previous step.
   - 2.e Store the resulting five values to the memory locations A_{i_1}, A_{i_2}, A_{i_3}, A_{i_4}, A_{i_5}.
3. Read the contents in the memory locations A_1, A_2, ..., A_M as measurements $\boldsymbol{y}$ of $\boldsymbol{x}$, and stop.

Computational resources and computational effort required for the implementation of (1) based on the above procedure are summarized in the first rows of Tables I and II. $\{A_1, A_2, \ldots, A_M\}$ is called as the data memory and $\{a_{j,i}\}$ for $i = 1, 2, 3, 4, 5$ and $j = 1, 2, \ldots, N$ is called as the address memory. Five adders are required for the implementation of Step 2.d of the above procedure. Complexity for the circuit shown in Fig. 1 is shown in the second rows of Tables I and II. As can be seen, the feature computation operation can be implemented using three memory locations for storing data, two adders, and one maximum value selector. Thus, additional computational resources required for the implementation of the proposed method in the bio-sensor hardware can be expected to be very small relative to that required for a typical implementation

of the CS operation. Computational effort, i.e., the number of mathematical operations required for the computation of features, is also significantly smaller than that required for the CS operation, see Table II.

TABLE I
COMPUTATIONAL RESOURCES FOR CS AND f_1, f_2 COMPUTATION

	Data memory	Address memory	Adders	Max. Selector
CS	M	MN	5	–
f_1, f_2	3	–	2	1

TABLE II
COMPUTATIONAL EFFORT FOR CS AND f_1, f_2 COMPUTATION

	Number of Operations			
	Addition	Memory Access	Max. Selector	ABS
CS	$5N$	$3 \times (5N)$	–	–
f_1, f_2	$2N$	–	N	N

IV. SIMULATION RESULTS

ECG signal from the first channel in the record `100m` downloaded from MIT-BIH Arrhythmia database [14] was preprocessed by applying the first two steps, namely, mean subtraction step and fifth-order moving average filtering step, used in [4] [15]. The ECG signal was of length 650000 samples (approx. 30 min.), and it was divided into a total of 2539 segments each of length 256. Features f_1 and f_2 were computed for each segment, and data matrix $\mathbf{T}$ of size 2539×2 was constructed by including features $\{f_1\}$ and $\{f_2\}$ for 2539 segments in the 1st and 2nd columns, respectively. All the segments were observed manually, and it was found that a total of 2335 segments contained QRS complexes, and 204 segments did not contain QRS complex. The QRS ECG segments were labelled as 0 and non-QRS ECG segments were labelled as 1. A label vector $\boldsymbol{g}$ of length 2539 was constructed by using the labels corresponding to the rows of $\mathbf{T}$ as its components.

1) Classification and cross validation (CV): Leave-one-out CV was used to evaluate the performance of the classifier. For $i = 1, 2, \ldots, 2539$: the ith row of $\mathbf{T}$ and the ith component of $\boldsymbol{g}$ were used as the test data. Rest of the rows of $\mathbf{T}$ and components of $\boldsymbol{g}$ were used as the training data. Support-vector machine (SVM) with linear and radial basis kernels, decision tree (DT), and linear discriminant analysis (LDA) were used for classification. Simulation was conducted in the R programming environment, and functions `svm`, `ctree`, and `lda` available in the packages `e1071`, `partykit`, and `lda`, respectively, were used for training the four classification models SVM (linear), SVM (radial basis), DT, and LDA. The generic function `predict` was used for the classification of the test data. Confusion matrices obtained for the five models are shown in Table III. Sensitivity, specificity, and area under the ROC curve (AUC) are shown in Table IV. As can be seen, the sensitivity, specificity, and AUC are highest for SVM.

In the proposed system, it is very important to minimize the error of classifying ECG segments with QRS complexes (label "0") as non-QRS ECG segment (label "1"). This situation of minimal *false positive* helps to minimize the number of ECG segments with QRS complexes that will be replaced by the zero vector. The confusion matrices in Table III show that the number of true "0"s that are predicted as "1" is 0 for SVM (radial basis) and 1 for SVM (linear), see bottom-left cell in the matrices. This is also reflected in the values of specificity, which is inversely related to number of false positives, shown in Table IV. This indicates that SVM would be effective for minimizing QRS misses.

TABLE III
CONFUSION MATRIX

	True 0	True 1
Predicted 0	2334	3
Predicted 1	1	201

(a) SVM (linear kernel)

	True 0	True 1
Predicted 0	2335	4
Predicted 1	0	200

(b) SVM (radial basis kernel)

	True 0	True 1
Predicted 0	2332	6
Predicted 1	3	198

(c) Decision Tree

	True 0	True 1
Predicted 0	2332	4
Predicted 1	3	200

(d) LDA

TABLE IV
SENSITIVITY, SPECIFICITY, AND AUC

	Sensitivity	Specificity	AUC
SVM (linear)	0.9853	0.9996	0.9924
SVM (radial basis)	0.9804	1.000	0.9902
Decision Tree	0.9706	0.9987	0.9974
LDA	0.9510	0.9996	0.9753

A. Computational Complexity

Mean and variance of the CPU times required for a total of 2539 instances of learning and classification are shown in Table V. As can be seen, the average amount of time required to learn SVM (radial basis) is the largest and that for LDA is the smallest. For classification, SVM and RF are the most efficient.

TABLE V
COMPUTATIONAL COMPLEXITY IN SECONDS

	Model learning		Segment classification	
	Mean	Variance	Mean	Variance
SVM (linear)	0.0176	2.4342e-05	0.0007	1.4608e-06
SVM (radial basis)	0.0393	1.5580e-05	0.0008	4.4337e-07
Dec. Tree	0.0124	2.3908e-05	0.0020	2.2046e-06
LDA	0.0095	1.0186e-05	0.0012	4.2322e-07

Five-fold cross validation was conducted, and temporal stability was also tested by using the ECG segments for the first 10 min. for training and that for the last 10 min. for testing. In both the cases, the results were same as that shown in Tables IV and V.

The $\ell^d_{2/p}$-RLS [9], ℓ^d_p-RLS [13], and ℓ^{2d}_p-RLS [11] algorithms were applied for the reconstruction of all 2539 ECG

segments from their measurements obtained with compression ratio of 95%, i.e., with the number of measurements $M = round(256/10) = 26$. Mean and variance of the computational effort (CPU time) for the $\ell^d_{2/p}$-RLS, ℓ^d_p-RLS, and ℓ^{2d}_p-RLS algorithms over 2539 reconstructions are shown in Table VI. As can be seen, the classification time of 0.7 and 0.8 millisec. for SVM (radial) and SVM (linear), respectively, shown in Table V is much smaller than the signal reconstruction time for the $\ell^d_{2/p}$-RLS, ℓ^d_p-RLS, and ℓ^{2d}_p-RLS algorithms shown in Table VI. Moreover, the results indicate that the $\ell^d_{2/p}$-RLS algorithm took approximately $200 \times 0.1824 = 36.48$ sec. for the reconstruction of 200 ECG segments that were detected by SVM(radial basis) as non-QRS ECG segments, see Table III. This amount of time would be saved from the total computational effort for a total of 2539 reconstructions, which is approximately $2539 \times 0.1824 = 463.11$ sec.

TABLE VI

SIGNAL RECONSTRUCTION COMPLEXITY

Algorithm	Mean (sec.)	Variance
$\ell^d_{2/p}$-RLS	0.1824	4.52e-3
ℓ^d_p-RLS	0.2050	2.48e-4
ℓ^{2d}_p-RLS	0.2312	3.28e-4

B. Alternative Circuit for Feature Computation

The `Select Maximum` operation in Fig. 1 would typically involve (a) computation of 2's complement of an input number, (b) addition of the two numbers, and (c) use of the resulting carry-over bit to determine the greater input number. Alternatively, the `Select Maximum` operation can be replaced by a parallel OR (or bitwise OR) operation, at the expense of a small amount of specificity. Sensitivity, specificity, and AUC obtained after making this replacement are shown in Table VII. As can be seen, there is a slight reduction in the specificity and slight increment in the sensitivity, relative to the results shown in Table IV. Reduction in specificity indicates that the bitwise OR operation slightly increases the number of false positives. The increase in the sensitivity indicates that the bitwise OR operation slightly decreases *false negatives*, i.e., the number of non-QRS ECG segments detected as that with the QRS complex. This would increase the number of applications of the signal reconstruction algorithm, thereby increase a small amount of computational complexity for the proposed method. Overall, AUC for SVM and LDA in Table VII is slightly more than that in Table IV.

TABLE VII

SENSITIVITY, SPECIFICITY, AND AUC FOR OR OPERATION FOR MAX. ABS. VALUE

	Sensitivity	Specificity	AUC
SVM (linear)	0.9902	0.9983	0.9942
SVM (radial basis)	0.9902	0.9983	0.9942
Decision Tree	0.9804	0.9996	0.9971
LDA	0.9902	0.9940	0.9921

V. CONCLUSIONS

An efficient method for the reconstruction of ECG segments for compressive sensing is proposed. The method is based on using a simple and efficient circuit for the computation of the sum of absolute differences and maximum value of absolute differences in the sensor, and using these values as features for the detection of QRS complex in the ECG segment. A machine learning-based classification can be used for segment detection. Zero vectors are used as the ECG segments detected as non-QRS ECG segments, thus saving the computation effort of signal reconstruction. Simulation results indicate that the proposed method can offer upto 7.4% reduction of signal reconstruction time.

ACKNOWLEDGMENT

The authors would like to thank Canada Research Chairs (CRC) program for supporting this research.

REFERENCES

[1] V. Goudar and M. Potkonjak, "Fault-tolerant and low-power sampling schedules for localized BASNs," *IEEE J. Emerg. Sel. Topic Circuits Syst.*, vol. 3, no. 1, pp. 86–95, Mar. 2013.

[2] H. Noshadi, et al., "HERMES: mobile system for instability analysis and balance assessment," *ACM Trans. Embedd. Comput. Syst.*, vol. 12, no. 1s, Mar. 2013.

[3] C. J. Deepu and Y. Lian, "A joint QRS detection and data compression scheme for wearable sensors," *IEEE Trans. Biomed. Eng.*, vol. 62, no. 1, Jan. 2015.

[4] G. Nallathambi and J. C. Principe, "Integrate and fire pulse train automation for QRS detection," *IEEE Trans. Biomed. Eng.*, vol. 61, no. 2, Feb. 2014.

[5] E. J. Candés and M. B. Wakin, "An introduction to compressive sampling," *IEEE Signal Process. Mag.*, vol. 25, no. 2, pp. 21–30, Mar. 2008.

[6] S. S. Chen, D. L. Donoho, and M. A. Saunders, "Atomic decomposition by basis pursuit," *SIAM J. Scientif. Comput.*, vol. 20, no. 1, pp. 33–61, 1999.

[7] J. K. Pant, W.-S. Lu, and A. Antoniou, "New improved algorithms for compressive sensing based on ℓ_p norm," *IEEE Trans. Circuits Syst. II*, vol. 61, no. 3, pp. 198–202, Mar. 2014.

[8] H. Mamaghanian, et al., "Compressed sensing for real-time energy-efficient ECG compression on wireless body sensor nodes," *IEEE Trans. Biomed. Eng.*, vol. 58, no. 9, pp. 2456–2466, Sep. 2011.

[9] J. K. Pant and S. Krishnan, "Compressive sensing of foot gait signals and its application for the estimation of clinically relevant time series," *IEEE Trans. Biomed. Eng. (accepted)*, 2015.

[10] Z. Zhang et al., "Compressed sensing for energy-efficient wireless telemonitoring of noninvasive fetal ECG via block sparse Bayesian learning," *IEEE Trans. Biomed. Eng.*, vol. 60, no. 2, pp. 300–309, Feb. 2013.

[11] J. K. Pant and S. Krishnan, "Compressive sensing of electrocardiogram signals by promoting sparsity on the second-order difference and by using dictionary learning," *IEEE Trans. Biomed. Circuits Syst.*, vol. 8, no. 2, pp. 293–302, Apr. 2014.

[12] B. Liu, et al., "Energy efficient telemonitoring of physiological signals via compressed sensing: a fast algorithm and power consumption evaluation," *Biomedical Signal Processing and Control*, vol. 11, pp. 80–88, 2014.

[13] J. K. Pant and S. Krishnan, "Reconstruction of ECG signals for compressive sensing by promoting sparsity on the gradient," in *Proc. IEEE Inter. Conf. Acoustics, Speech, and Signal Process.*, May 2013, pp. 993–997.

[14] Physionet: MIT-BIH arrhythmia database. [Online]. Available: http://www.physionet.org/physiobank/database/mitdb/

[15] A. Amann, R. Tratnig, and K. Unterkofler, "Reliability of old and new ventricular fibrillation detection algorithms for automated external defibrillators," *Biomed. Eng. Online*, vol. 4, no. 60, Oct. 2005.